Journal of Photochemistry and Photobiology A: Chemistry 203 (2009) 177–185

Contents lists available at ScienceDirect

Journal of Photochemistry and Photobiology A: Chemistry

journal homepage: www.elsevier.com/locate/jphotochem

Photovoltaic performance of dye-sensitized solar cells based on a series of new-type donor–acceptor π-conjugated sensitizer, benzofuro[2,3-*c*]oxazolo[4,5-*a*]carbazole fluorescent dyes

Yousuke Ooyama, Yoshihito Shimada, Akihiro Ishii, Genta Ito, Yusuke Kagawa, Ichiro Imae, Kenji Komaguchi, Yutaka Harima*

Department of Applied Chemistry, Graduate School of Engineering, Hiroshima University, 1-4-1 Kagamiyama, Higashi-hiroshima 739-8527, Japan

ARTICLE INFO

Article history:
Received 26 September 2008
Received in revised form 8 January 2009
Accepted 27 January 2009
Available online 7 February 2009

Keywords:
Heterocycles
Dye sensitized solar cells
Fluorescence
Donor–acceptor π-conjugated fluorophores

ABSTRACT

A series of new-type donor–acceptor π-conjugated benzofuro[2,3-*c*]oxazolo[4,5-*a*]carbazole fluorescent dyes with substituents such as various lengths of non-conjugated alkyl chains containing a carboxyl group at the end position, π-conjugated carboxyl, cyano and dibutylamino groups are designed and synthesized. Dye-sensitized solar cells were fabricated using these dyes. The influence of configuration of the dyes on TiO_2 surface and chemical structures of the dyes on the photovoltaic performance are investigated and discussed on the basis of semi-empirical molecular orbital calculations (AM1 and INDO/S). It is concluded that a carboxyl group of donor–acceptor π-conjugated sensitizer is necessary not as the electron acceptor, but only as anchoring group for attachment on TiO_2 surface. Therefore, it was proposed that the most important point for developing new and efficient donor–acceptor π-conjugated sensitizers for DSSCs is to design dye molecules capable of forming a strong interaction between the electron acceptor moiety of sensitizers and TiO_2 surface.

1. Introduction

Dye-sensitized solar cells (DSSCs) based on organic dyes have received considerable attention because of high incident solar light-to-electricity conversion efficiency and low cost of production [1–20]. A large number of organic dyes have been developed and the relationship between the chemical structure and photovoltaic performance of DSSCs based on the dyes is examined. Donor–acceptor π-conjugated organic dyes possessing broad and intense spectral features are especially useful as sensitizers. Furthermore, the charge recombination of the injected electron in metal oxide with donor–acceptor π-conjugated dyes was an order of magnitude slower than for comparable dyes that lacked the electron donor groups, because spatial separation of the positive charge density on donor moiety of the oxidized dye (excited dye) and the injected electrons has the crucial effect of retarding the rate of charge recombination between the injected electrons and the oxidized dye. The charge recombination with the oxidized dye is a key loss mechanism of DSSCs [2,21–26]. Many donor–acceptor π-conjugated dyes with carboxyl group, acting as not only anchoring group for attachment on metal oxide but also the electron acceptor, have been synthesized and used as sensitizers of DSSCs [2–20]. A number of studies have suggested that a carboxyl group can form an ester linkage with TiO_2 surface to provide a strongly bound dye and a good electron communication between them. However, development of new donor–acceptor π-conjugated dyes for DSSCs is limited because a carboxyl group is required to combine with π-conjugation system or electron acceptor moiety of dyes for the above reasons.

In our previous study, to clarify the influence of the position of a carboxyl group attached to the same chromophore skeleton on photovoltaic performances of DSSCs, we have designed and synthesized novel donor–acceptor π-conjugated benzofuro[2,3-*c*]oxazolo[4,5-*a*]carbazole-type fluorescent dyes **1b**, **3c**, **5a** and **5b** (Scheme 1), where the electron acceptor is a carboxyl group for **1b** and a cyano group for **3c**, **5a** and **5b** [27]. The photovoltaic performance of **3c** having a non-conjugated linkage between a carboxyl group and a chromophore is similar to that of **1a** and higher than those of **5a** and **5b**. To understand the differences in the photovoltaic performance, it was assumed that the dye **3c** is standing perpendicularly to the TiO_2 substrate as shown in Fig. 1, and that the dye **3c** can efficiently inject electrons from the phenylcyano group to the conduction band of TiO_2 electrode through an intermolecular hydrogen bonding between a cyano nitrogen of the dye and a hydroxyl proton of the TiO_2 surface.

Quite recently, in order to provide a further confirmation for this view, we have designed and synthesized donor–acceptor π-conjugated benzofuro[2,3-*c*]oxazolo[4,5-*a*]carbazole fluorescent dyes **3a**–**3f** with different lengths of non-conjugated alkyl chains

* Corresponding author. Fax: +81 82 424 5494.
E-mail address: harima@mls.ias.hiroshima-u.ac.jp (Y. Harima).

1010-6030/$ – see front matter © 2009 Elsevier B.V. All rights reserved.
doi:10.1016/j.jphotochem.2009.01.017

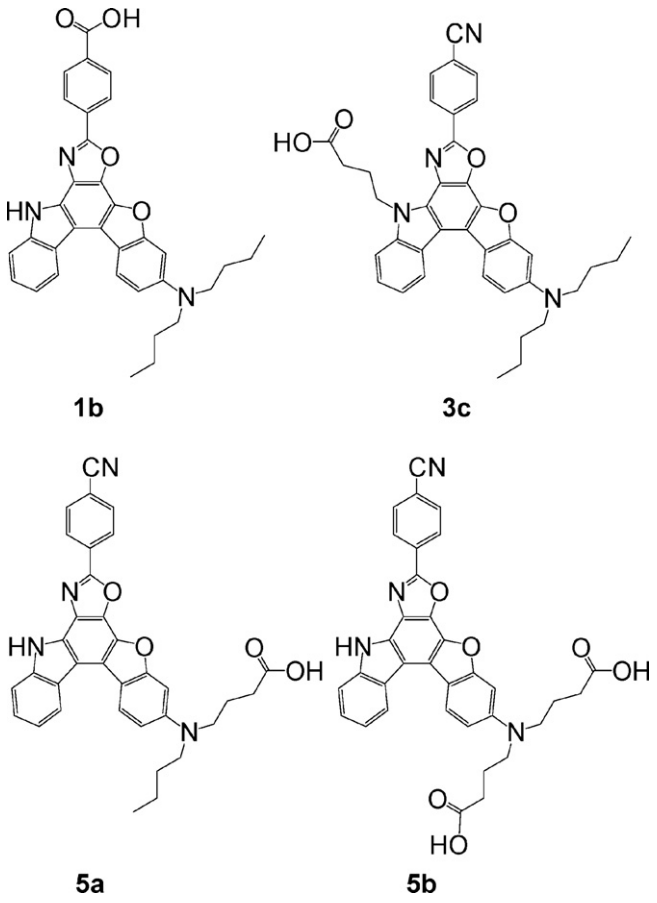

Scheme 1. Chemical structures of benzofuro[2,3-*c*]oxazolocarbazole-type fluorescent dyes.

containing a carboxyl group at the end position and their photovoltaic performances of dye-sensitized solar cells are investigated [28]. It is found that in spite of the lengths of the alkyl chains, due to flexibility of alkyl chain, the cyano group of the dyes is located in close proximity to TiO_2 surface and thus a good electron communication between the dyes and TiO_2 surface is established (Fig. 1). It is concluded that a carboxyl group of donor–acceptor π-conjugated sensitizer is necessary not as the electron acceptor, but only as anchoring group for attachment on TiO_2 surface.

In this work, we have designed and synthesized donor–acceptor π-conjugated sensitizers with two carboxyl groups, benzofuro[2,3-*c*]oxazolo[4,5-*a*]carbazole fluorescent dyes **4c** and **4f**. It is very useful for development of new and efficient donor–acceptor π-conjugated sensitizers to obtain information of the photovoltaic performances by comparing donor–acceptor π-conjugated sensitizers having two carboxyl groups with those having a carboxyl group. Here we report photovoltaic performances of DSSCs based on the fluorescent dyes **1b**, **3a**–**3f**, **4c**, and **4f** and discuss the influence of configuration of the dye on TiO_2 surface and chemical structures of the dyes on the photovoltaic performance on the basis of semi-empirical molecular orbital calculations (AM1 and INDO/S).

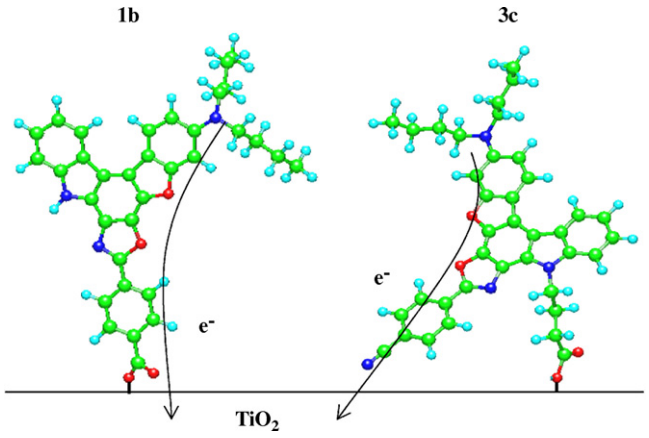

Fig. 1. Plausible configurations of **1b** and **3c** on TiO_2 surface.

2. Experimental

Melting points were measured with a Yanaco micro melting point apparatus MP model. IR spectra were recorded on a Perkin Elmer Spectrum One FT-IR spectrometer by ATR method. Absorption spectra were observed with a Shimadzu UV-3150 spectrophotometer and fluorescence spectra were measured with a Hitachi F-4500 spectrophotometer. The fluorescence quantum yields (Φ) were determined by a Hamamatsu C9920-01 equipped with CCD by using a calibrated integrating sphere system (λ_{ex} = 325 nm). Cyclic voltammograms (CVs) were recorded in $MeCN/Et_4NClO_4$ (0.1 M) solution with a three-electrode system consisting of Ag/Ag^+ as reference electrode, Pt plate as working electrode, and Pt wire as counter electrode, by using a Hokuto Denko HAB-151 potentiostat equipped with a functional generator. Elemental analyses were recorded on a Perkin Elmer 2400 II CHN analyzer. ^1H NMR spectra were recorded on a JNM-LA-400 (400 MHz) FT NMR spectrometer with tetramethylsilane (TMS) as an internal standard. Column chromatography was performed on silica gel (KANTO CHEMICAL, 60N, spherical, neutral).

2.1. Synthesis of 7-(4-cyanophenyl)-3-dibutylamino-benzofuro [2,3-c]oxazolo[4,5-a]carbazole, 9-acetic acid ethyl ester (**2a**)

A solution of **1a** (1.0 g, 1.90 mmol) in dry acetonitrile was treated with sodium hydride (60%, 0.11 g, 2.85 mmol) and stirred for 1 h at room temperature. Ethyl bromoacetate (1.59 g, 9.49 mmol) was added in dropwise manner over 20 min and the solution was stirred at room temperature for 2 h. After concentrating under reduced pressure, the resulting residue was dissolved in CH_2Cl_2, and washed with water. The organic extract was dried over $MgSO_4$, filtered, and concentrated. The residue was chromatographed on silica gel (CH_2Cl_2 as eluent) to give **2a** (0.84 g, yield 72%): Mp. 247–249 °C; IR (ATR): $\tilde{\nu}$ = 2222, 1739 cm^{-1}; ^1H NMR (400 MHz, acetone[D_6], TMS) δ = 1.04 (t, 6H), 1.24 (t, 3H), 1.46–1.54 (m, 4H), 1.70–1.78 (m, 4H), 3.49–3.54 (t, 4H), 4.19–4.24 (m, 2H), 5.74 (s, 2H), 6.95–7.00 (m, 2H), 7.44–7.48 (m, 1H), 7.54–7.58 (m, 1H), 7.71–7.73 (m, 1H), 8.03–8.05 (m, 2H), 8.47–8.50 (m, 3H), 8.69–8.70 (m, 1H); elemental analysis calcd (%) for $C_{38}H_{36}N_4O_4$: C 74.49, H 5.92, N 9.14; found: C 74.85, H 6.00, N 9.01.

2.2. Synthesis of 7-(4-cyanophenyl)-3-dibutylamino-benzofuro [2,3-c]oxazolo[4,5-a]carbazole, 9-acetic acid (**3a**)

To a solution of **2a** (0.1 g, 0.16 mmol) in ethanol (500 ml) was added dropwise aqueous NaOH (0.07 g, 1.6 mmol, 20 mL), with stirring at 60 °C. After further stirring for 3 h under reflux, the solution was acidified to pH 4 with 2N HCl, and concentrated under reduced pressure. The residue was dissolved in CH_2Cl_2, and washed with water. The organic extract was dried over $MgSO_4$, filtered, and concentrated. The residue was chromatographed on silica gel (CH_2Cl_2 as eluent) to give **3a** (0.053 g, yield 54%): Mp. 279–281 °C; IR (ATR): $\tilde{\nu}$ = 2226, 1707 cm^{-1}; ^1H NMR (400 MHz, acetone[D_6], TMS) δ = 1.04 (t, 6H), 1.47–1.53 (m, 4H), 1.70–1.75 (m, 4H), 3.51–3.55 (m, 4H), 5.64

(s, 2H), 7.00–7.04 (m, 2H), 7.45–7.48 (m, 1H), 7.56–7.60 (m, 1H), 7.88–7.90 (m, 1H), 8.06–8.08 (m, 2H), 8.48–8.54 (m, 3H), 8.70–8.71 (m, 1H). MS (EI, *m*/*z*) 584 (M^+).

2.3. Synthesis of 7-(4-cyanophenyl)-3-dibutylamino-benzofuro [2,3-c]oxazolo[4,5-a]carbazole, 9-propionic acid ethyl ester (**2b**)

A solution of **1a** (1.0 g, 1.90 mmol) in dry acetonitrile was treated with sodium hydride (60%, 0.11 g, 2.85 mmol) and stirred for 1 h at room temperature. Ethyl 3-bromopropionate (1.72 g, 9.49 mmol) was added in dropwise manner over 20 min and the solution was stirred at room temperature for 1 h. After concentrating under reduced pressure, the resulting residue was dissolved in CH_2Cl_2, and washed with water. The organic extract was dried over $MgSO_4$, filtered, and concentrated. The residue was chromatographed on silica gel (CH_2Cl_2 as eluent) to give **2b** (0.46 g, yield 39%): Mp. 205–207 °C; IR (ATR): $\tilde{\nu} = 2229$, 1725 cm^{-1}; ^1H NMR (400 MHz, acetone[D_6], TMS) δ = 1.04 (t, 6H), 1.10 (t, 3H), 1.47–1.53 (m, 4H), 1.71–1.74 (m, 4H), 3.13 (t, 2H), 3.50–3.55 (m, 4H), 4.01–4.07 (m, 2H), 5.26 (t, 2H), 6.98–7.02 (m, 2H), 7.42–7.45 (m, 1H), 7.56–7.60 (m, 1H), 7.84–7.86 (m, 1H), 8.06–8.08 (m, 2H), 8.50–8.53 (m, 3H), 8.68–8.70 (m, 1H); elemental analysis calcd (%) for $C_{39}H_{38}N_4O_4$: C 74.74, H 6.11, N 8.38; found: C 74.58, H 6.16, N 8.62.

2.4. Synthesis of 7-(4-cyanophenyl)-3-dibutylamino-benzofuro [2,3-c]oxazolo[4,5-a]carbazole, 9-propionic acid (**3b**)

To a solution of **2b** (0.1 g, 0.16 mmol) in ethanol (500 ml) was added dropwise aqueous NaOH (0.06 g, 1.6 mmol, 30 mL), with stirring at 60 °C. After further stirring for 2 h under reflux, the solution was acidified to pH 4 with 2N HCl, and concentrated under reduced pressure. The residue was dissolved in CH_2Cl_2, and washed with water. The organic extract was dried over $MgSO_4$, filtered, and concentrated. The residue was chromatographed on silica gel (CH_2Cl_2:ethyl acetate = 5:1 as eluent) to give **3b** (0.025 g, yield 25%): Mp. 264–266 °C; IR (ATR): $\tilde{\nu} = 2228$, 1767 cm^{-1}; ^1H NMR (400 MHz, DMSO[D_6], TMS) δ = 0.96 (t, 6H), 1.35–1.43 (m, 4H), 1.57–1.64 (m, 4H), 3.35–3.50 (t, 4H) overlap peak of dissolved water in DMSO[d_6], 2.93–2.96 (t, 2H), 5.12 (t, 2H), 6.93 (dd, *J* = 2.20 and 8.28 Hz, 1H), 7.02 (d, *J* = 2.20 Hz, 1H), 7.37–7.41 (m, 1H), 7.52–7.56 (m, 1H), 7.84 (d, *J* = 8.28 Hz, 1H), 8.08 (d, *J* = 8.56 Hz, 2H), 8.35 (d, *J* = 8.56 Hz, 2H), 8.44 (d, *J* = 8.80 Hz, 1H), 8.59 (d, *J* = 8.52 Hz, 1H). MS (EI, *m*/*z*) 598 (M^+).

2.5. Synthesis of 7-(4-cyanophenyl)-3-dibutylamino-benzofuro [2,3-c]oxazolo[4,5-a]carbazole, 9-butyric acid ethyl ester (**2c**)

A solution of **1a** (1.0 g, 1.90 mmol) in dry acetonitrile was treated with sodium hydride (60%, 0.11 g, 2.85 mmol) and stirred for 1 h at room temperature. Ethyl 4-bromobutyrate (1.85 g, 9.49 mmol) was added in dropwise manner over 20 min and the solution was stirred at room temperature for 10 h. After concentrating under reduced pressure, the resulting residue was dissolved in CH_2Cl_2, and washed with water. The organic extract was dried over $MgSO_4$, filtered, and concentrated. The residue was chromatographed on silica gel (CH_2Cl_2 as eluent) to give **2c** (0.77 g, yield 63%); Mp. 209–211 °C; IR (ATR): $\tilde{\nu} = 2228$, 1738 cm^{-1}; ^1H NMR (400 MHz, acetone[D_6], TMS) δ = 1.04 (t, 6H), 1.12 (t, 3H), 1.48–1.52 (m, 4H), 1.71–1.76 (m, 4H), 1.89–1.92 (m, 2H), 2.46–2.50 (m, 2H), 3.51–3.54 (m, 4H), 4.00–4.04 (m, 2H), 5.07–5.11 (m, 2H), 7.00–7.04 (m, 2H), 7.39–7.46 (m, 1H), 7.53–7.60 (m, 1H), 7.81–7.86 (m, 1H), 8.04–8.08 (m, 2H), 8.51–8.58 (m, 3H), 8.70–8.74 (m, 1H); elemental analysis calcd (%) for $C_{40}H_{40}N_4O_4$: C 74.98, H 6.29, N 8.74; found: C 74.97, H 6.31, N 8.71.

2.6. Synthesis of 7-(4-cyanophenyl)-3-dibutylamino-benzofuro [2,3-c]oxazolo[4,5-a]carbazole, 9-butyric acid (**3c**)

To a solution of **2c** (0.1 g, 0.16 mmol) in ethanol (300 ml) was added dropwise aqueous NaOH (0.06 g, 1.6 mmol, 30 mL), with stirring at 60 °C. After further stirring for 6 h under reflux, the solution was acidified to pH 4 with 2N HCl, and concentrated under reduced pressure. The residue was dissolved in CH_2Cl_2, and washed with water. The organic extract was dried over $MgSO_4$, filtered, and concentrated. The residue was chromatographed on silica gel (CH_2Cl_2:ethyl acetate = 10:1 as eluent) to give **3c** (0.085 g, yield 89%): Mp. 260–262 °C; IR (ATR): $\tilde{\nu} = 2228$, 1712 cm^{-1}; ^1H NMR (400 MHz, acetone[D_6], TMS) δ = 1.04 (t, 6H), 1.46–1.53 (m, 2H), 1.74–1.79 (m, 4H), 1.88–1.91 (m, 4H), 3.51–3.55 (m, 2H), 3.61–3.64 (m, 4H), 5.11–5.15 (m, 2H), 6.98–7.05 (m, 2H), 7.43–7.46 (m, 1H), 7.56–7.60 (m, 1H), 7.85 (d, *J* = 8.76 Hz, 1H), 8.07 (d, *J* = 8.76 Hz, 2H), 8.54 (d, *J* = 9.04 Hz, 2H), 8.59 (d, *J* = 8.80 Hz, 1H), 8.73 (d, *J* = 8.08 Hz, 1H); elemental analysis calcd (%) for $C_{38}H_{36}N_4O_4$: C 74.49, H 5.92, N 9.14; found: C 74.29, H 5.83, N 9.09.

2.7. Synthesis of 7-(4-cyanophenyl)-3-dibutylamino-benzofuro [2,3-c]oxazolo[4,5-a]carbazole, 9-pentanoic acid ethyl ester (**2d**)

A solution of **1a** (1.0 g, 1.90 mmol) in dry acetonitrile was treated with sodium hydride (60%, 0.11 g, 2.85 mmol) and stirred for 1 h at room temperature. Ethyl 5-bromovalerate (1.99 g, 9.49 mmol) was added in dropwise manner over 20 min and the solution was stirred at room temperature for 5 h. After concentrating under reduced pressure, the resulting residue was dissolved in CH_2Cl_2, and washed with water. The organic extract was dried over $MgSO_4$, filtered, and concentrated. The residue was chromatographed on silica gel (CH_2Cl_2 as eluent) to give **2d** (0.93 g, yield 74%): Mp. 168–170 °C; IR (ATR): $\tilde{\nu} = 2226$, 1730 cm^{-1}; ^1H NMR (400 MHz, acetone[D_6], TMS) δ = 1.05 (t, 6H), 1.11 (t, 3H), 1.47–1.55 (m, 4H), 1.71–1.79 (m, 6H), 2.01–2.10 (m, 2H) overlap peak of remained acetone, 2.40–2.44 (m, 2H), 3.50 (t, 4H), 3.99–4.03 (m, 2H), 4.88 (t, 2H), 6.94–6.96 (m, 2H), 7.38–7.42 (m, 1H), 7.52–7.56 (m, 1H), 7.72–7.74 (m, 1H), 7.96 (d, *J* = 8.80 Hz, 2H), 8.38 (d, *J* = 8.80 Hz, 2H), 8.42 (d, *J* = 9.76 Hz, 1H), 8.62 (d, *J* = 8.56 Hz, 1H); elemental analysis calcd (%) for $C_{41}H_{42}N_4O_4$: C 75.20, H 6.47, N 8.56; found: C 75.13, H 6.56, N 8.34.

2.8. Synthesis of 7-(4-cyanophenyl)-3-dibutylamino-benzofuro [2,3-c]oxazolo[4,5-a]carbazole, 9-pentanoic acid (**3d**)

To a solution of **2d** (0.1 g, 0.15 mmol) in ethanol (500 ml) was added dropwise aqueous NaOH (0.06 g, 1.6 mmol, 10 mL), with stirring at 60 °C. After further stirring for 6 h under reflux, the solution was acidified to pH 4 with 2N HCl, and concentrated under reduced pressure. The residue was dissolved in CH_2Cl_2, and washed with water. The organic extract was dried over $MgSO_4$, filtered, and concentrated. The residue was chromatographed on silica gel (CH_2Cl_2 as eluent) to give **3d** (0.039 g, yield 39%): Mp. 229–231 °C; IR (ATR): $\tilde{\nu} = 2226$, 1716 cm^{-1}; ^1H NMR (400 MHz, DMSO[D_6], TMS) δ = 0.97 (t, 6H), 1.35–1.43 (m, 4H), 1.59–1.64 (m, 6H), 1.91–2.00 (m, 2H), 2.28–2.31 (m, 2H), 3.35–3.50 (t, 4H) overlap peak of dissolved water in DMSO[D_6], 4.92 (t, 2H), 6.92 (dd, *J* = 2.20 and 8.28 Hz, 1H), 7.00 (d, *J* = 2.20 Hz, 1H), 7.37–7.41 (m, 1H), 7.53–7.57 (m, 1H), 7.80 (d, *J* = 8.28 Hz, 1H), 8.08 (d, *J* = 8.28 Hz, 2H), 8.38 (d, *J* = 8.28 Hz, 2H), 8.43 (d, *J* = 9.28 Hz, 1H), 8.60 (d, *J* = 7.84 Hz, 1H); elemental analysis calcd (%) for $C_{39}H_{38}N_4O_4$: C 74.74, H 6.11, N 8.94; found: C 74.48, H 6.41, N 8.55.

2.9. Synthesis of 7-(4-cyanophenyl)-3-dibutylamino-benzofuro [2,3-c]oxazolo[4,5-a]carbazole, 9-haxanoic acid ethyl ester (**2e**)

A solution of **1a** (1.0 g, 1.90 mmol) in dry acetonitrile was treated with sodium hydride (60%, 0.11 g, 2.85 mmol) and stirred for 1 h

at room temperature. Ethyl 6-bromohexanoate (2.12 g, 9.49 mmol) was added in dropwise manner over 20 min and the solution was stirred at room temperature for 12 h. After concentrating under reduced pressure, the resulting residue was dissolved in CH_2Cl_2, and washed with water. The organic extract was dried over $MgSO_4$, filtered, and concentrated. The residue was chromatographed on silica gel (CH_2Cl_2 as eluent) to give **2e** (0.96 g, yield 76%): Mp. 181–182 °C; IR (ATR): $\tilde{\nu} = 2227$, 1731 cm^{-1}; ^1H NMR (400 MHz, acetone[D_6], TMS) $\delta = 1.05$ (t, 6H), 1.14 (t, 3H), 1.45–1.61 (m, 6H), 1.71–1.80 (m, 6H), 2.01–2.10 (m, 2H) overlap peak of remained acetone, 2.28–2.32 (m, 2H), 3.53 (t, 4H), 4.01–4.06 (m, 2H), 4.99 (t, 2H), 6.98–7.01 (m, 2H), 7.41–7.44 (m, 1H), 7.54–7.58 (m, 1H), 7.77–7.79 (m, 1H), 8.03–8.05 (m, 2H), 8.49–8.53 (m, 3H), 8.69–8.71 (n, 1H); elemental analysis calcd (%) for $C_{42}H_{44}N_4O_4$: C 75.42, H 6.63, N 8.38; found: C 74.99, H 6.58, N 8.26.

2.10. Synthesis of 7-(4-cyanophenyl)-3-dibutylamino-benzofuro [2,3-c]oxazolo[4,5-a]carbazole, 9-haxanoic acid (*3e*)

To a solution of **2e** (0.1 g, 0.15 mmol) in ethanol (500 ml) was added dropwise aqueous NaOH (0.06 g, 1.6 mmol, 30 mL), with stirring at 60 °C. After further stirring for 6 h under reflux, the solution was acidified to pH 4 with 2N HCl, and concentrated under reduced pressure. The residue was dissolved in CH_2Cl_2, and washed with water. The organic extract was dried over $MgSO_4$, filtered, and concentrated. The residue was chromatographed on silica gel (CH_2Cl_2 as eluent) to give **3e** (0.062 g, yield 63%): Mp. 214–215 °C; IR (ATR): $\tilde{\nu} = 2225$, 1704 cm^{-1}; ^1H NMR (400 MHz, DMSO[D_6], TMS) $\delta = 0.97$ (t, 6H), 1.36–1.44 (m, 6H), 1.59–1.64 (m, 6H), 1.92–1.98 (m, 2H), 2.18–2.25 (m, 2H), 3.35–3.50 (t, 4H) overlap peak of dissolved water in DMSO[D_6], 4.92 (t, 2H), 6.93 (dd, $J = 1.68$ and 8.04 Hz, 1H), 7.01 (d, $J = 1.68$ Hz, 1H), 7.37–7.41 (m, 1H), 7.53–7.57 (m, 1H), 7.80 (d, $J = 8.04$ Hz, 1H), 8.08 (d, $J = 8.78$ Hz, 2H), 8.38 (d, $J = 8.78$ Hz, 2H), 8.44 (d, $J = 9.52$ Hz, 1H), 8.60 (d, $J = 8.32$ Hz, 1H); elemental analysis calcd (%) for $C_{40}H_{40}N_4O_4$: C 74.98, H 6.29, N 8.74; found: C 74.86, H 6.33, N 8.71.

2.11. Synthesis of 7-(4-cyanophenyl)-3-dibutylamino-benzofuro [2,3-c]oxazolo[4,5-a]carbazole, 9-heptanoic acid ethyl ester (*2f*)

A solution of **1a** (1.0 g, 1.90 mmol) in dry acetonitrile was treated with sodium hydride (60%, 0.11 g, 2.85 mmol) and stirred for 1 h at room temperature. Ethyl 7-bromoheptanoate (2.25 g, 9.49 mmol) was added in dropwise manner over 20 min and the solution was stirred at room temperature for 12 h. After concentrating under reduced pressure, the resulting residue was dissolved in CH_2Cl_2, and washed with water. The organic extract was dried over $MgSO_4$, filtered, and concentrated. The residue was chromatographed on silica gel (CH_2Cl_2:ethyl acetate = 5:1 as eluent) to give **2f** (0.89 g, yield 69%): Mp. 201–203 °C; IR (ATR): $\tilde{\nu} = 2227$, 1727 cm^{-1}; ^1H NMR (400 MHz, $CDCl_3$, TMS) $\delta = 1.02$ (t, 6H), 1.22 (t, 3H), 1.40–1.71 (m, 14H), 2.03–2.11 (m, 2H), 2.27 (t, 2H), 3.43 (t, 4H), 4.06–4.11 (m, 2H), 4.99 (t, 2H), 6.92–6.99 (m, 2H), 7.40–7.44 (m, 1H), 7.54–7.63 (m, 2H), 7.85–7.89 (m, 2H), 8.46–8.51 (m, 3H), 8.66–8.68 (m, 1H); elemental analysis calcd (%) for $C_{43}H_{46}N_4O_4$: C 75.63, H 6.79, N 8.20; found: C 75.87, H 6.78, N 8.20.

2.12. Synthesis of 7-(4-cyanophenyl)-3-dibutylamino-benzofuro [2,3-c]oxazolo[4,5-a]carbazole, 9-heptanoic acid (*3f*)

To a solution of **2f** (0.1 g, 0.15 mmol) in ethanol (300 ml) was added dropwise aqueous NaOH (0.06 g, 1.6 mmol, 30 mL), with stirring at 60 °C. After further stirring for 12 h under reflux, the solution was acidified to pH 4 with 2N HCl, and concentrated under reduced pressure. The residue was dissolved in CH_2Cl_2, and washed with water. The organic extract was dried over $MgSO_4$, filtered, and concentrated. The residue was chromatographed on silica gel (CH_2Cl_2:ethyl acetate = 3:2 as eluent) to give **3f** (0.076 g, yield 77%): Mp. 195–197 °C; IR (ATR): $\tilde{\nu} = 2226$, 1707 cm^{-1}; ^1H NMR (400 MHz, $CDCl_3$, TMS) $\delta = 1.02$ (t, 6H), 1.41–1.68 (m, 14H), 2.02–2.06 (m, 2H), 2.34 (t, 2H), 3.43 (t, 4H), 4.92 (t, 2H), 6.79–6.94 (m, 2H), 7.38–7.41 (m, 1H), 7.52–7.61 (m, 2H), 7.81–7.83 (m, 2H), 8.39–8.41 (m, 3H), 8.63–8.65 (m, 1H); elemental analysis calcd (%) for $C_{41}H_{42}N_4O_4$: C 75.20, H 6.47, N 8.56; found: C 74.88, H 6.45, N 8.46.

2.13. Synthesis of 7-(4-carboxyphenyl)-3-dibutylamino-benzofuro[2,3-c]oxazolo[4,5-a]carbazole, 9-butyric acid (*4c*)

To a solution of **2c** (0.3 g, 0.47 mmol) in ethanol (500 ml) was added dropwise aqueous NaOH (0.19 g, 4.7 mmol, 30 mL), with stirring under reflux. After further stirring for 24 h under reflux, the solution was acidified to pH 4 with 2N HCl, and concentrated under reduced pressure. The residue was dissolved in CH_2Cl_2, and washed with water. The organic extract was dried over $MgSO_4$, filtered, and concentrated. The residue was chromatographed on silica gel (CH_2Cl_2:methanol = 5:1 as eluent) to give **4c** (0.059 g, yield 20%); 280–282 °C (decomposition); IR (ATR): $\tilde{\nu} = 1708$, 1678 cm^{-1}; ^1H NMR (400 MHz, DMSO[D_6], TMS) $\delta = 0.99$ (t, 6H), 1.40–1.44 (m, 4H), 1.59–1.64 (m, 4H), 2.21–2.24 (m, 2H), 2.36 (t, 2H), 3.51 (t, 4H), 5.00 (t, 2H), 6.92–7.04 (m, 2H), 7.40–7.42 (m, 1H), 7.55–7.57 (m, 1H), 7.83 (d, $J = 8.29$ Hz, 1H), 8.15 (d, $J = 8.05$ Hz, 2H), 8.38 (d, $J = 7.56$ Hz, 2H), 8.45 (d, $J = 8.54$ Hz, 1H), 8.62 (d, $J = 7.08$ Hz, 1H). MS (MALDI, m/z) 631 (M^+).

2.14. Synthesis of 7-(4-carboxyphenyl)-3-dibutylamino-benzofuro[2,3-c]oxazolo[4,5-a]carbazole, 9-heptanoic acid (*4f*)

To a solution of **2f** (0.3 g, 0.44 mmol) in ethanol (500 ml) was added dropwise aqueous NaOH (0.18 g, 4.4 mmol, 30 mL), with stirring under reflux. After further stirring for 12 h under reflux, the solution was acidified to pH 4 with 2N HCl, and concentrated under reduced pressure. The residue was dissolved in CH_2Cl_2, and washed with water. The organic extract was dried over $MgSO_4$, filtered, and concentrated. The residue was chromatographed on silica gel (CH_2Cl_2:methanol = 5:1 as eluent) to give **4f** (0.142 g, yield 46%): Mp. 218–220 °C; IR (ATR): $\tilde{\nu} = 1687$ cm^{-1}; ^1H NMR (400 MHz, DMSO[D_6], TMS) $\delta = 0.99$ (t, 6H), 1.37–1.47 (m, 10H), 1.60–1.64 (m, 4H), 1.95–1.98 (m, 2H), 2.18 (t, 2H), 3.43 (t, 4H), 4.99 (t, 2H), 6.95–7.06 (m, 2H), 7.39–7.43 (m, 1H), 7.55–7.58 (m, 1H), 7.84 (d, $J = 8.29$ Hz, 1H), 8.16 (d, $J = 8.54$ Hz, 2H), 8.37 (d, $J = 8.05$ Hz, 2H), 8.48 (d, $J = 9.76$ Hz, 1H), 8.64 (d, $J = 7.81$ Hz, 1H) (MALDI, m/z) 673 (M^+).

2.15. Computational methods

The semi-empirical calculations were carried out with the WinMOPAC Ver. 3.9 package (Fujitsu, Chiba, Japan). Geometry calculations in the ground state were made using the AM1 method [29]. All geometries were completely optimized (keyword PRECISE) by the eigenvector following routine (keyword EF). Experimental absorption spectra of the eight compounds were compared with their absorption data by the semi-empirical method INDO/S (intermediate neglect of differential overlap/spectroscopic) [30–32]. All INDO/S calculations were performed using single excitation full SCF/CI (self-consistent field/configuration interaction), which includes the configuration with one electron excited from any occupied orbital to any unoccupied orbital, where 225 configurations were considered [keyword CI (15 15)].

2.16. Preparation of the dye-sensitized solar cells

The TiO_2 electrodes used for dye-sensitized solar cells were prepared as follows. Into a powder (1.30 g) of TiO_2 (P-25, $d = 30$–40 nm)

in mortar was added water (1.9 mL) in six portions with well stirring. Then, three drops of 12 M nitric acid and polyethylene glycol (80 mg) were successively added, and the mixture was well kneaded to a smooth paste. It was then applied on a fluorine-doped-tin-oxide (FTO) substrate and sintered for 30 min at 500 °C. The 7 μm thick TiO_2 electrode (0.5 × 0.5 cm^2 in photoactive area) was immersed into a 0.3 mM tetrahydrofuran solution of the dye for a number of hours enough to adsorb the photosensitizer. The DSSCs were fabricated by using the dye-adsorbed TiO_2 electrode thus prepared, Pt-coated glass as a counter electrode, and a solution of 0.05 M iodine, 0.1 M lithium iodide, and 1,2-dimethyl-3-*n*-propylimidazolium iodide in acetonitrile as electrolyte. The photocurrent–voltage characteristics were measured using a potentiostat under a simulated solar light (AM 1.5, 61 mW cm^{-2}). IPCE spectra were measured under monochromatic irradiation with a tungsten-halogen lamp and a monochromator. The dye-coated film was immersed in mixture solvent of THF-DMSF-1 M NaOH aq (5: 4: 1), which was used to determine the amount of dye molecule adsorbed onto the film by measuring the absorbance. The quantification of each dye was made based on the λ_{max} and the molar extinction coefficient of each dye in the above solution. Absorption spectra of the dye-adsorbed TiO_2 films adsorbed by dyes were measured in the diffuse-reflection mode by a Shimadzu UV-3150 spectrophotometer with a calibrated integrating sphere system ISR-3100.

3. Results and discussion

3.1. Synthesis of benzofuro[2,3-c]oxazolo[4,5-a]carbazole-type fluorescent dyes

The synthetic pathway of benzofuro[2,3-*c*]oxazolo[4,5-*a*]carbazole-type fluorescent dyes **3a**–**3f**, **4c**, and **4f** is shown in Scheme 2. We used compound **1a** as a starting material [33,34]. The reaction of **1a** with alkylhalide using sodium hydride yielded **2a**–**2f**. The hydrolysis of **2a**–**2f** in the presence of NaOH at 60 °C and under reflux gave the compounds **3a**–**3f** and **4c** and **4f**, respectively.

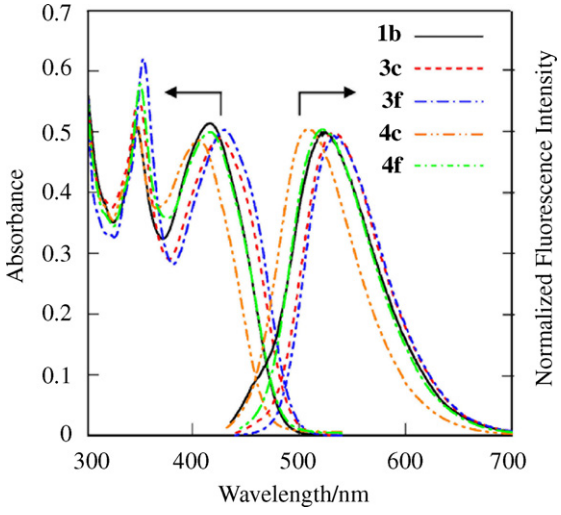

Fig. 2. Absorption and fluorescence spectra of **1b**, **3c**, **3f**, **4c**, and **4f** in 1,4-dioxane.

3.2. Spectroscopic properties of the fluorescent dyes *1b*, *3a*–*3f*, *4c*, and *4f* in solution and on TiO_2 film

The absorption and fluorescence spectra of **1b**, **3c**, **3f**, **4c**, and **4f** in 1,4-dioxane are shown in Fig. 2 and the spectral data for all dyes are summarized in Table 1. All these fluorescent dyes exhibit intense absorption bands at around 411–431 and 347–354 nm, and an intense fluorescence at around 515–540 nm. The fluorescence quantum yields (Φ) of these dyes in 1,4-dioxane are close to 100%. The absorption and fluorescence spectra of all these fluorescent dyes resemble very well, showing that the effect of phenylcyano and phenylcarboxy substituents on photophysical properties of these dyes is negligible, although the absorption and fluorescence maxima of **1b**, **4c**, and **4f** are slightly blue-shifted compared to those of **3a**–**3f**. Absorption spectra of dyes adsorbed on TiO_2 film are shown in Fig. 3, where the amounts of adsorbed dyes are

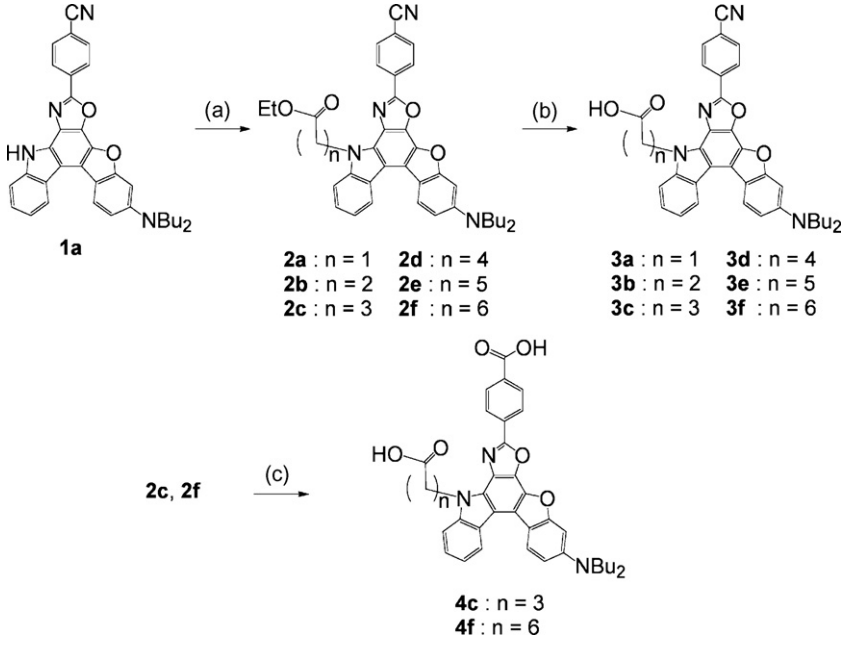

Scheme 2. Synthesis of fluorescent dyes **2a**–**2f**, **3a**–**3f**, **4c**, and **4f**: (a) NaH, alkylhalide, acetonitrile, R.T., 1–12 h, 72% for **2a**, 39% for **2b**, 63% for **2c**, 74% for **2d**, 76% for **2e**, and 69% for **2f**; (b) NaOH aq, ethanol, 60 °C, 2–12 h, 54% for **3a**, 25% for **3b**, 89% for **3c**, 39% for **3d**, 63% for **3e**, and 77% for **3f**; (c) NaOH aq, ethanol, reflux, 2–3 days, 20% for **4c** and 46% for **4f**.

Table 1
Optical properties of **1b**, **3a**–**3f**, **4c**, and **4f** in 1,4-dioxane.

Dye	λ_{max}^{abs}/nm (ε_{max}/dm^3 mol^{-1} cm^{-1})[a]	λ_{max}^{fl}/nm[b]	Φ	SS[c]/nm
1b	416 (25700), 347 (25400)	525	0.97	109
3a	427 (26700), 350 (26100)	540	0.97	113
3b	425 (25300), 350 (26900)	532	0.96	107
3c	425 (24400), 349 (27300)	537	0.99	112
3d	430 (26900), 354 (33000)	534	0.97	104
3e	430 (28900), 354 (35000)	534	0.95	104
3f	431 (26100), 354 (31000)	533	0.95	103
4c	411 (24300), 348 (25500)	515	0.95	104
4f	417 (21100), 350 (24500)	522	0.97	105

[a] 2.0×10^{-5} M.
[b] 2.0×10^{-6} M.
[c] Stokes shift value.

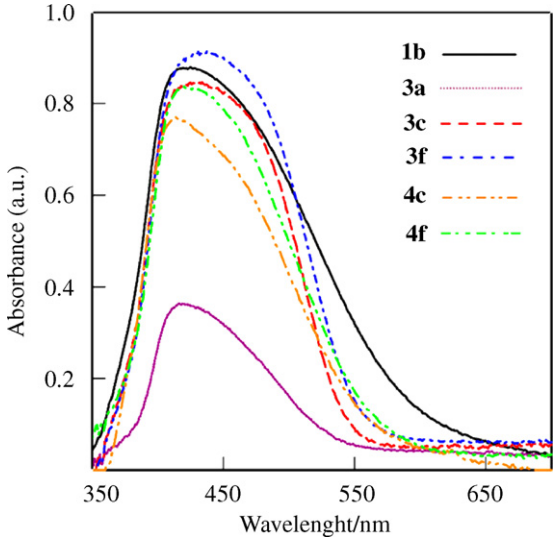

Fig. 3. Absorption spectra of **1b**, **3a**, **3c**, **3f**, **4c**, and **4f** adsorbed on TiO_2 film, measured in the diffuse-reflection mode (Shimadzu UV-3150, ISR-3100).

6.8×10^{16}, 4.4×10^{15}, 6.6×10^{16}, 5.5×10^{16}, 7.8×10^{16}, 7.2×10^{16}, 7.4×10^{16}, 6.0×10^{16}, and 6.5×10^{16} molecules cm^{-2} for **1b**, **3a**–**3f**, **4c**, and **4f**, respectively. The absorbance and absorption peak wavelengths of adsorbed dyes on TiO_2 films are very similar to one another, but only the absorbance of **3a** is lower than those of the other dyes. Undoubtedly, the low absorbance of **3a** is ascribable to the small amount of **3a** adsorbed on TiO_2 film. In all the dyes except **3a**, the onsets of absorption bands of adsorbed dyes are red-shifted by 80–100 nm relative to those in 1,4-dioxane. Such a red-shift is attributable to aggregation of the dyes on TiO_2 electrode [11,20,35,36].

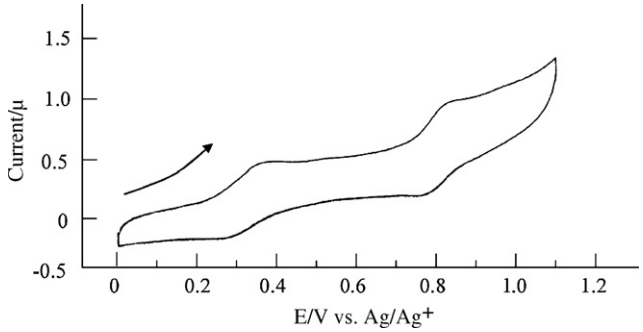

Fig. 4. Cyclic voltammogram of **3e** in acetonitrile containing 0.1 M Et_4NClO_4 at a scan rate of 20 mV s^{-1}. The arrow denotes the direction of the potential scan.

3.3. *Electrochemical properties of the fluorescent dyes **1b**, **3a**–**3f**, **4c**, and **4f** and their HOMO and LUMO energy levels*

The electrochemical properties of **1b**, **3a**–**3f**, **4c**, and **4f** were determined by cyclic voltammetry (CV) in acetonitrile containing 0.1 M Et_4NClO_4. As an example, the CV of **3e** is shown in Fig. 4. The CV data are summarized in Table 2. The first oxidation peaks were determined to be 0.31–0.36 V *vs.* Ag/Ag$^+$. The corresponding reduction peaks appeared at 0.25–0.31 V. The first redox waves are clearly observed and the peak separations are ca. 60 mV, suggesting that the first oxidized states of the dyes are stable. On the other hand, ill-defined waves for the second and third oxidation processes indicate that the second and third oxidized states of the dyes are less stable than the first ones.

On the basis of the spectral analyses and CVs, we estimated the HOMO energy levels of these dyes with respect to NHE. The LUMO energy levels of the dyes were estimated from the first oxidation potential and an intersection of absorption and fluorescence spectra (487–460 nm (2.54–2.70 eV) for **1b**, **3a**–**3f**, **4c**, and **4f**) corresponding to the energy gap between HOMO and LUMO (Table 2). The results of absorption and fluorescence spectra and CV for these dyes demonstrate that all these dyes have similar HOMO and LUMO energy levels. Evidently, the LUMO energy levels for these dyes are higher than the energy level of TiO_2 conduction band (−0.5 V), showing that these dyes can inject efficiently electrons to conduction band of TiO_2 electrode.

3.4. *Semi-empirical MO calculations (AM1, INDO/S)*

To understand the photophysical and electrochemical properties of benzofuro[2,3-*c*]oxazolo[4,5-*a*]carbazole-type fluorescent dyes, we carried out semi-empirical molecular orbital (MO) calculations of **1b**, **3a**–**3f**, **4c**, and **4f** by the INDO/S method after geometrical optimizations by the MOPAC/AM1 method [29–32]. The calculated absorption wavelengths and the transition char-

Table 2
Electrochemical properties of **1b**, **3a**–**3f**, **4c**, and **4f** and their energy levels of HOMO and LUMO.

Dye	E_{pa}/V *vs.* Ag/Ag$^+$[a]	E_{pc}/V *vs.* Ag/Ag$^+$[a]	ΔE_p/mV	$E_{1/2}$/V	HOMO/V[b]	LUMO/V[b]
1b	0.31, 0.82, 0.98	0.25, –, –	60, –, –	0.28, –, –	0.87	−1.71
3a	0.35, 0.88, –	0.29, 0.81, –	60, 70, –	0.32, 0.85, –	0.87	−1.71
3b	0.36, 0.85, –	0.31, 0.80, –	50, 50, –	0.34, 0.83, –	0.90	−1.70
3c	0.35, 0.84, 0.98	0.28, 0.78, –	70, 60, –	0.32, 0.81, –	0.91	−1.64
3d	0.35, 0.85, –	0.30, 0.79, –	50, 60, –	0.33, 0.82, –	0.89	−1.66
3e	0.36, 0.83, –	0.29, 0.77, –	70, 60, –	0.33, 0.80, –	0.89	−1.66
3f	0.33, 0.82, –	0.27, 0.76, –	60, 60, –	0.30, 0.79, –	0.86	−1.75
4c	0.35, 0.80, –	0.30, 0.72, –	50, 80, –	0.33, 0.76, –	0.91	−1.79
4f	0.33, 0.89, –	0.28, –, –	50, –, –	0.31, –, –	0.89	−1.65

[a] E_{pa} and E_{pc} are the anodic and cathodic peak potentials in acetonitrile (0.1 M Et_4NClO_4).
[b] *vs.* a normal hydrogen electrode (NHE).

Table 3
Calculated absorption spectra for **1b**, **3a**–**3f**, **4c**, and **4f**.

Compound	Absorption (calc.)		CI component[b]
	λ_{max}/nm	f[a]	
1b	402	0.92	HOMO → LUMO(75%)
	328	0.59	HOMO → LUMO+1(43%)
			HOMO-1 → LUMO(13%)
3a	396	0.92	HOMO → LUMO(76%)
	326	0.60	HOMO → LUMO+1(40%)
			HOMO-1 → LUMO(14%)
3b	403	0.91	HOMO → LUMO(77%)
	329	0.64	HOMO → LUMO+1(44%)
			HOMO-1 → LUMO(17%)
3c	404	0.90	HOMO → LUMO(77%)
	329	0.64	HOMO → LUMO+1(47%)
			HOMO-1 → LUMO(16%)
3d	402	0.92	HOMO → LUMO(77%)
	329	0.63	HOMO → LUMO+1(44%)
			HOMO-1 → LUMO(16%)
3e	404	0.91	HOMO → LUMO(77%)
	329	0.64	HOMO → LUMO+1(46%)
			HOMO-1 → LUMO(17%)
3f	403	0.92	HOMO → LUMO(78%)
	329	0.63	HOMO → LUMO+1(45%)
			HOMO-1 → LUMO(16%)
4c	405	0.87	HOMO → LUMO(75%)
	329	0.51	HOMO → LUMO+1(33%)
			HOMO-1 → LUMO(13%)
4f	406	0.88	HOMO → LUMO(76%)
	330	0.54	HOMO → LUMO+1(36%)
			HOMO-1 → LUMO(14%)

[a] Oscillator strength.
[b] The transition is shown by an arrow from one orbital to another, followed by its percentage CI (configuration interaction) component.

acters of the first absorption bands are collected in Table 3. The observed and calculated absorption spectra of the compounds (Tables 1 and 3) compare well with each other with respect to both the absorption wavelength and the absorption intensity, although the calculated absorption wavelengths are blue-shifted. The deviation of the INDO/S calculations, giving transition energies greater than the experimental values, has been generally observed [37,38]. The calculations showed that the longest excitation bands of the dyes were mainly assigned to the transition from HOMO to LUMO, where HOMOs were mostly localized on the 3-dibutylamino-benzofuro[2,3-*c*]oxazolo[4,5-*a*]carbazole moiety for all dyes, and LUMOs were mostly localized on the carboxyphenyl moiety for **1b**, **4c**, and **4f** and the cyanophenyl moiety for **3a**–**3f**. The changes in the calculated electron density accompanying the first electron excitation are shown in Fig. 5, which reveals a strong intramolecular charge migration from the

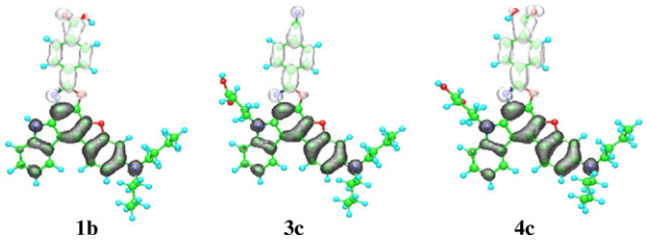

Fig. 5. Calculated electron density changes accompanying the first electronic excitation of **1b**, **3c**, and **4c**. The black and white lobes signify decrease and increase in electron density accompanying the electronic transition. Their areas indicate the magnitude of the electron density change.

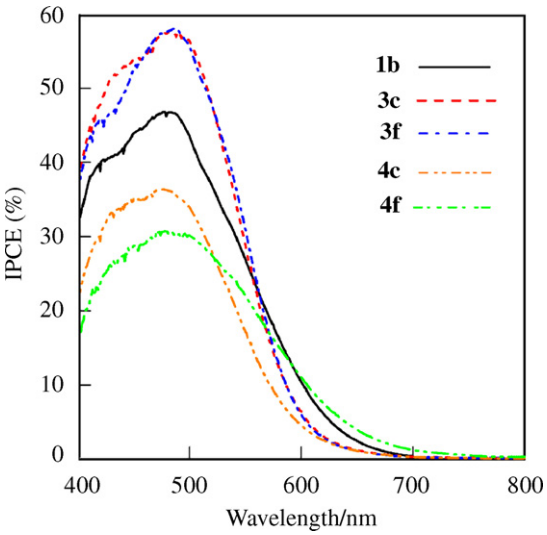

Fig. 6. IPCE spectra of DSSCs based on **1b**, **3c**, **3f**, **4c**, and **4f**.

3-dibutylamino-benzofuro[2,3-*c*]oxazolo[4,5-*a*]carbazole moiety to the carboxylphenyl or cyanophenyl moiety for all dyes. These calculation results suggest that the effects of the cyano and carboxyl groups on photophysical and electrochemical properties of these dyes are negligible, so that all dyes show similar results of the absorption and fluorescence spectra and the CV.

3.5. *Photovoltaic performances of DSSCs based on the fluorescent dyes **1b**, **3a**–**3f**, **4c**, and **4f***

The DSSCs were fabricated by using the dye-adsorbed TiO_2 electrode, Pt-coated glass as a counter electrode, and an acetonitrile solution with 0.05 M iodine, 0.1 M lithium iodide, and 1,2-dimethyl-3-*n*-propylimidazolium iodide as electrolyte. The photocurrent–voltage characteristics were measured using a potentiostat under a simulated solar light (AM 1.5, 61 mW cm^{-2}). The incident photon-to-current conversion efficiency (IPCE) spectra were measured under monochromatic irradiation with a tungsten-halogen lamp and a monochromator. IPCE spectra and photocurrent–voltage curves are depicted in Figs. 6 and 7,

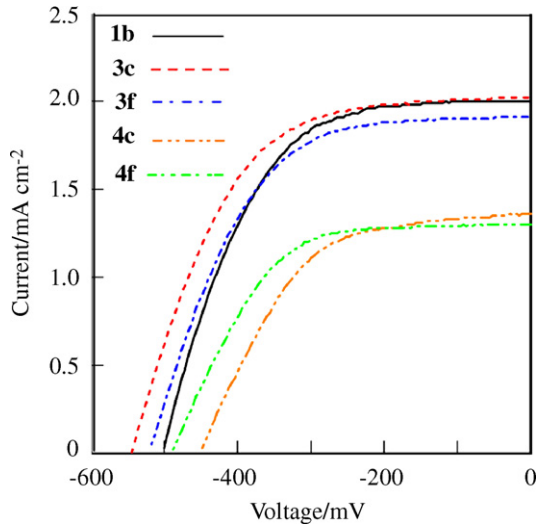

Fig. 7. Photocurrent–voltage curves of DSSCs based on **1b**, **3c**, **3f**, **4c**, and **4f**.

Table 4
Photovoltaic performances of DSSCs based on **1b**, **3a**–**3f**, **4c**, and **4f**.

Dye	Molecules cm^{-2} [a]	J_{sc}/mA cm^{-2}	V_{oc}/mV	*ff*	η (%)
1b	6.8×10^{16}	2.12	508	0.57	1.00
3a	4.4×10^{15}	0.12	216	0.42	0.02
3b	6.6×10^{16}	2.06	500	0.57	1.00
3c	5.5×10^{16}	2.01	548	0.56	1.00
3d	7.8×10^{16}	1.88	524	0.53	0.86
3e	7.2×10^{16}	2.00	468	0.55	0.84
3f	7.4×10^{16}	1.91	520	0.57	0.90
4c	6.0×10^{16}	1.36	448	0.55	0.55
4f	6.5×10^{16}	1.30	488	0.59	0.61

[a] Adsorption amount per unit area of TiO_2 film.

respectively. The IPCE is represented by the following equation:

$$\mathrm{IPCE}(\%) = \frac{1240(\mathrm{eV\ nm})J_{sc}(\mathrm{mA\ cm^{-2}})}{\lambda(\mathrm{nm})\Phi(\mathrm{mW\ cm^{-2}})} \times 100 \quad (1)$$

where J_{sc} is the short-circuit photocurrent density generated by monochromatic light, and λ and Φ are the wavelength and the intensity of the monochromatic light, respectively. When the performances of DSSCs fabricated using these dyes as sensitizers were examined, big differences in the IPCE spectra and the photocurrent–voltage (*I*–*V*) characteristics were observed (Figs. 6 and 7). The maximum IPCE value increases in the order of **3b**–**3f** (52–58%) > **1b** (46%) > **4c**, **4f** (36, 31%). Table 4 summarizes photovoltaic performances of DSSCs based on the dyes. The solar energy-to-electricity conversion yield (η (%)) is expressed by the following equation:

$$\eta(\%) = \frac{J_{sc}(\mathrm{mA\ cm^{-2}})V_{oc}(\mathrm{V})ff}{I_0(\mathrm{mW\ cm^{-2}})} \times 100 \quad (2)$$

where I_0 is the intensity of incident white light, V_{oc} is the open-circuit photovoltage, and *ff* represents the fill factor. Interestingly, the J_{sc} for **3b**–**3f** (1.88–2.06 mA cm^{-2}) having a nonconjugated linkage between carboxyl group and chromophore is similar to that for **1b** (2.12 mA cm^{-2}) and higher than those of **4c** (1.36 mA cm^{-2}) and **4f** (1.30 mA cm^{-2}) with two carboxyl groups. However, although the maximum IPCE value of **1b** is lower than those of **3c** and **3f**, the J_{sc} for **1b** is similar to those for **3c** and **3f**, because the IPCE spectrum of **1b** extends to the longer wavelength region; the onset of IPCE spectrum for **1b** is 700 nm which is red-shifted by about 20 nm compared to those of **3c** and **3f** (Fig. 6). The η values increase in the order of **1b** (1.00%) ≥ **3b**–**3f** (0.84–1.00%) > **4c**, **4f** (0.55, 0.61%) ≫ **3a** (0.02%). The photovoltaic performance of **3a** is lower than those for the other dyes. The values of V_{oc} for **1b**, **3a**, **3b**–**3f**, **4c**, and **4f** are 508, 216, 468–548, 448, and 488 mV, respectively, which were different among the dyes.

3.6. Consideration of relationship between photovoltaic performances and configuration of dye on TiO_2 surface

To understand the differences in J_{sc} and η, we assumed that the dye molecule is standing perpendicular to the TiO_2 substrate as shown in Fig. 1. In **1b**, a carboxyl group can form an ester linkage with TiO_2 surface, so that electrons will be injected from dye to TiO_2 through a carboxyl group. For **3b**–**3f**, on the other hand, a carboxyl group acts as an anchoring group for attachment on TiO_2 surface, but it cannot participate in the path of electrons because of a non-conjugated alkyl chains between a carboxyl group and a chromophore. From the molecular structure of **3b**–**3f**, it was suggested that phenylcyano group acting as electron acceptor is located in close proximity to TiO_2 surface by the interaction such as intermolecular hydrogen bonding between cyano nitrogen of the dye and hydroxyl proton of TiO_2 surface. In view of highly efficient charge injection probabilities as suggested by IPCE values over 50% for **3b**–**3f**, it is likely that the electron-accepting phenylcyano groups are attached to the TiO_2 as shown in Fig. 1, so that the dyes **3b**–**3f** can efficiently inject electrons from the dye skeleton to the conduction band of the TiO_2 through the phenylcyano groups. Consequently, the close agreements of all the photovoltaic features for **3b**–**3f** demonstrate that the π-conjugated skeletons of these dyes lie on the TiO_2 surface in a similar fashion irrespective of different lengths of alkyl chains with a carboxyl group acting as an anchor. Fukuzumi et al. reported that for DSSC based on fluorescein derivatives, the xanthen moiety acting as an electron acceptor which can inject electrons to the conduction band of the semiconductor, is located in close proximity to the semiconductor surface [39]. The lower photovoltaic performance of **3a** is attributable to the small amount of **3a** adsorbed on TiO_2 film compared with those for the other dyes because of a steric hindrance between the phenylcyano moiety of **3a** and TiO_2 surface. On the other hand, it was expected that the dyes **4c** and **4f** with two carboxyl groups can form strong interaction with TiO_2 surface, so that electrons will be injected from dye to TiO_2 through carboxyl group in carboxyphenyl moiety, similar to **1b**. However, the J_{sc} values of **4c** and **4f** are smaller than that of **1b**. It was considered that strong interaction with TiO_2 surface for **4c** and **4f** induce the charge recombination between the injected electron and the oxidized dye (excited dye), which was faster than for comparable dyes that have a carboxyl group because of close approach of the oxidized **4c** and **4f** to TiO_2 surface. Otsubo et al. reported that for DSSC based on oligothiophenedicarboxylic acid with two carboxyl groups at both ends of oligothiophene skeleton, the dicarboxylated groups force molecular arrangements close to the TiO_2 electrode, resulting in the lowering of photovoltages due to enhanced quenching process [40]. Tian and co-workers have also reported that stronger adsorption of the dye with two carboxyl groups on the TiO_2 surface could facilitate charge recombination of the injected electron and oxidized dye [26]. Consequently, it is reasonable to presume that low photovoltaic performance for **4c** and **4f** are ascribable to the charge recombination between the injected electron and the oxidized dye. On the other hand, the values of V_{oc} were different among the dyes. It is reported that the Fermi level of TiO_2 is affected by adsorption of dyes having permanent dipoles: the dipole of dye can affect the electronic state of TiO_2 conduction band [41]. The direction of dipole moment of the dyes **1b**, **3a**–**3f**, **4c**, and **4f** in the adsorption state will be different among the dyes because of different positions of carboxyl groups on a chromophore skeleton and the number of carboxyl groups. Thus, this will cause the difference of V_{oc}. The η values of DSSCs based on these dyes are relatively small compared with those of other organic dyes because the π-conjugated system of these dyes does not have an intense absorption band over a long-wavelength region of the solar spectrum.

4. Conclusions

We have designed and synthesized a series of new-type donor–acceptor π-conjugated benzofuro[2,3-*c*]oxazolo[4,5-*a*]carbazole fluorescent dyes with substituents such as various lengths of non-conjugated alkyl chains containing a carboxyl group at the end position, π-conjugated carboxyl, cyano and dibutylamino groups, and photovoltaic performances of DSSCs based on these dyes are investigated. It is concluded that a carboxyl group of donor–acceptor π-conjugated sensitizer is necessary not as the electron acceptor, but only as anchoring group for attachment on TiO_2 surface. Ultimately, the most important point for developing new and efficient donor–acceptor π-conjugated sensitizers for DSSCs is to design dye molecules capable of forming a strong interaction between the electron acceptor moiety of sensitizers and TiO_2 surface.

Acknowledgments

This work was supported by Grants-in-Aid for Scientific Research (B) (19350094) and for Young Scientist (B) (18750174 and 20750161) from the Ministry of Education, Science, Sports and Culture of Japan, and by Electric Technology Research Foundation of Chugoku.

References

[1] B. O'Regan, M. Gräetzel, Nature 353 (1991) 737.
[2] N. Robertson, Angew. Chem. Int. Ed. 45 (2006) 2338.
[3] Q.-H. Yao, F.-S. Meng, F.-Y. Li, H. Tian, C.-H. Haung, J. Mater. Chem. 13 (2003) 1048.
[4] Y.-S. Chen, C. Li, Z.-H. Zeng, W.-B. Wang, X.-S. Wang, B.-W. Zhang, J. Mater. Chem. 15 (2005) 246.
[5] K.R.J. Thomas, J.T. Lin, Y.-C. Hsu, K.-C. Ho, Chem. Commun. (2005) 4098.
[6] D.P. Hagberg, T. Edvinsson, T. Marinado, G. Boschloo, A. Hagfeld, L. Sun, Chem. Commun. (2006) 2245.
[7] S.-L. Li, K.-J. Jiang, K.-F. Shao, L.-M. Yang, Chem. Commun. (2006) 2792.
[8] T. Horiuchi, H. Miura, K. Sumioka, S. Uchida, J. Am. Chem. Soc. 126 (2004) 12218.
[9] K. Hara, K. Sayama, Y. Ohga, A. Shinpo, S. Suga, H. Arakawa, Chem. Commun. (2001) 569.
[10] K. Hara, M. Kurashige, S. Ito, A. Shinpo, S. Suga, K. Sayama, H. Arakawa, Chem. Commun. (2003) 252.
[11] K. Hara, M. Kurashige, Y. Dan-oh, C. Kasada, A. Shinpo, S. Suga, K. Sayama, H. Arakawa, New J. Chem. 27 (2003) 783.
[12] Z.-S. Wang, F.-Y. Li, C.-H. Hang, L. Wang, M. Wei, L.-P. Jin, N.-Q. Li, J. Phys. Chem. B 104 (2000) 9676.
[13] A. Ehret, L. Stuhl, M.T. Spitler, J. Phys. Chem. B 105 (2001) 9960.
[14] K. Hara, T. Sato, R. Katho, A. Furube, Y. Ohga, A. Shinpo, S. Suga, K. Sayama, H. Sugihara, H. Arakawa, J. Phys. Chem. B 107 (2003) 597.
[15] W. Zhan, W. Wu, J. Hua, Y. Jing, F. Meng, H. Tian, Tetrahedron Lett. 48 (2007) 2461.
[16] A. Burke, L. Schmidt-Mende, S. Ito, M. Grätzel, Chem. Commun. (2007) 234.
[17] D. Kim, J.K. Lee, S.O. Kang, J. Ko, Tetrahedron 63 (2007) 1913.
[18] H. Choi, J.K. Lee, K. Song, S.O. Kang, J. Ko, Tetrahedron 63 (2007) 3115.
[19] S. Kim, H. Choi, D. Kim, K. Song, S.O. Kang, J. Ko, Tetrahedron 63 (2007) 9206.
[20] Y. Ooyama, A. Ishii, Y. Kagawa, I. Imae, Y. Harima, New J. Chem. 31 (2007) 2076.
[21] J.N. Clifford, G. Yahioglu, L.R. Milgrom, J.R. Durrant, Chem. Commun. (2002) 1260.
[22] N. Hirata, J.-J. Lagref, E.J. Palomares, J.R. Durrant, M.K. Nazeeruddin, M. Grätzel, Chem. Eur. J. 10 (2004) 595.
[23] J.N. Clifford, E. Palomares, M.K. Nazeeruddin, M. Grätzel, J. Nelson, X. Li, N.J. Long, J.R. Durrant, J. Am. Chem. Soc. 126 (2004) 5225.
[24] S.A. Haque, S. Handa, K. Pater, E. Palomares, M. Thelakkat, J.R. Durrant, Angew. Chem. Int. Ed. 44 (2005) 5740.
[25] S. Handa, H. Wietasch, M. Thelakkat, J.R. Durrant, S.A. Haque, Chem. Commun. (2007) 1725.
[26] Q.-H. Yao, F.-H. Meng, F.-Y. Li, H. Tian, C.-H. Huang, J. Mater. Chem. 13 (2003) 1048.
[27] Y. Ooyama, Y. Shimada, Y. Kagawa, I. Imae, Y. Harima, Org. Biomol. Chem. 5 (2007) 2046.
[28] Y. Ooyama, Y. Shimada, Y. Kagawa, Y. Yamada, I. Imae, K. Komaguchi, Y. Harima, Tetrahedron Lett. 48 (2007) 9167.
[29] M.J.S. Dewar, E.G. Zoebisch, E.F. Healy, J.J. Stewart, J. Am Chem. Soc. 107 (1985) 389.
[30] J.E. Ridley, M.C. Zerner, Theor. Chim. Acta 32 (1973) 111.
[31] J.E. Ridley, M.C. Zerner, Theor. Chim. Acta 42 (1976) 223.
[32] A.D. Bacon, M.C. Zerner, Theor. Chim. Acta 53 (1979) 21.
[33] Y. Ooyama, Y. Harima, Chem. Lett. (2006) 902.
[34] Y. Ooyama, Y. Kagawa, Y. Harima, Eur. J. Org. Chem. 22 (2007) 3613.
[35] T. Horiuchi, H. Miura, S. Uchida, Chem. Commun. (2003) 3036.
[36] X.-H. Zhang, C. Li, W.-B. Wang, X.-X. Cheng, X.-S. Wang, B.-W. Zhang, J. Mater. Chem. 17 (2007) 642.
[37] M. Adachi, Y. Murata, S. Nakamura, J. Org. Chem. 58 (1993) 5238.
[38] W.M.F. Fabian, S. Schuppler, O.S. Wolfbesis, J. Chem. Soc. Perkin Trans. 2 (1996) 853.
[39] S. Hattori, T. Hasobe, K. Ohkubo, Y. Urano, N. Umezawa, T. Nagano, Y. Wada, S. Yanagida, S. Fukuzumi, J. Phys. Chem. B 108 (2004) 15200.
[40] K. Tanaka, K. Takimiya, T. Otsubo, K. Kawabuchi, S. Kajihara, Y. Harima, Chem. Lett. (2006) 592.
[41] S. Rühle, M. Greenshtein, S.-G. Chen, A. Merson, H. Pizem, C.S. Sukenik, D. Cahen, A. Zaban, J. Phys. Chem. B 109 (2005) 18907.